ELSEVIER

Marine Geology 245 (2007) 107–122

MARINE GEOLOGY
INTERNATIONAL JOURNAL OF MARINE GEOLOGY, GEOCHEMISTRY AND GEOPHYSICS

www.elsevier.com/locate/margeo

# Mass settling flux of fine sediments in Northern European estuaries: Measurements and predictions

A.J. Manning [a,b,*], K.R. Dyer [b]

[a] HR Wallingford Ltd, Estuaries and Dredging group, Howbery Park, Wallingford, Oxon, OX10 8BA, United Kingdom
[b] Coastal Processes Research Group, Marine Institute of the University of Plymouth, School of Earth, Ocean and Environmental Sciences, University of Plymouth, Portland Square Building, Drake Circus, Plymouth, Devon, PL4 8AA, United Kingdom

Received 5 April 2006; received in revised form 1 June 2007; accepted 5 July 2007

**Abstract**

This study describes a new flocculation model, which was based entirely on observations of settling floc spectra and turbulent shear stresses, acquired primarily from a series of in-situ experiments conducted in several European estuaries. The synthesis identified that the key components which best quantitatively describe a floc population are: the changes in the macrofloc (>160 μm) and microfloc settling velocities ($Ws_{macroEM}$ and $Ws_{microEM}$), together with how the suspended matter is distributed across each floc sub-population ($SPM_{ratioEM}$). The $Ws_{macroEM}$ algorithm displayed an increase in settling velocity at low shear stresses due to flocculation enhanced by shear, and floc disruption at higher stresses for the same concentration; the transition being a turbulent shear stress of about 0.36 N $m^{-2}$. The combination of the three algorithms into a single equation to predict mass settling flux ($MSF_{EM}$), estimated the total flux of the 157 measured floc samples with a cumulative error<4%. In comparison, the use of single Ws of 0.5 mm $s^{-1}$ and 5 mm $s^{-1}$ were both in error by an average of −86% and +41%, respectively. A concentration — settling parameterisation and the van Leussen techniques under-predicted the total cumulative flux by 35 and 38%, respectively. Furthermore, the analysis indicated that the various existing methods all incurred high predictive errors, at times under-estimating by over 70%, as concentration levels rose in close proximity to the bed. The findings of this study demonstrate the new Manning Floc Settling Velocity (MFSV) empirical model has flexibility in adapting to a wide range of both turbulent shear stress and suspended sediment concentration estuarine conditions.


*Keywords:* mass settling flux; flocculation; turbulent shear stress; macrofloc; settling velocity; suspended particulate matter; cohesive sediment; INSSEV instrument; parameterisation; numerical sediment transport models

## 1. Introduction

Predicting the transport and fate of sediment movement in estuaries requires the determination of various spatial and temporal mass fluxes. One problematic area is the accurate mathematical description of the vertical mass settling flux of cohesive sediment, which becomes the depositional flux close to slack water. This flux is the product of the suspended particulate matter

* Corresponding author. Coastal Processes Research Group, Marine Institute of the University of Plymouth, School of Earth, Ocean and Environmental Sciences, University of Plymouth, Portland Square Building, Drake Circus, Plymouth, Devon, PL4 8AA, United Kingdom. Fax: +44 752 232406.
*E-mail address:* andymanning@yahoo.com (A.J. Manning).

0025-3227/$ - see front matter © 2007 Elsevier B.V. All rights reserved.
doi:10.1016/j.margeo.2007.07.005

(SPM) concentration and the settling velocity. For non-cohesive sediment this is a relatively simple process, as the settling velocity is proportional to the square of the particle size. In contrast estuarine muds, which are composed of both clay minerals and biological matter, have the potential to flocculate into larger aggregates called flocs. As flocs grow in size they settle quicker, but become less dense and more porous. Also the rheological properties of suspended particulate matter are governed by volume concentrations, as opposed to mass concentrations (Dyer, 1989).

The rate of flocculation is a function of: SPM concentration, salinity, mineralogy, biological stickiness, and the physical mechanisms which bring the cohesive particles into contact (Manning, 2004a). van Leussen (1988) deduced that turbulent shear stresses, principally those generated by velocity gradients present in an estuarine water column, are the dominant particle collision mechanism. This mechanism was deemed most effective for turbulent shear stresses ranging between 0.03 and 0.8 N $m^{-2}$, which are representative of those typically experienced in the near-bed region of many Northern European macrotidal and mesotidal estuaries. Turbulent shear can promote floc growth, whilst high levels of turbulence can cause disruption to the flocculation process by instigating floc break-up, (McCave, 1984) which can lead to continual particle re-cycling and re-entrainment (Mehta and Partheniades, 1975).

The specification of the flocculation term within numerical models depends upon the sophistication of the model. The most simplistic parameterisation is a settling velocity value which remains constant in both time and space. These fixed settling values are typically selected on an arbitrary basis and adjusted by model calibration. The next step has been to use gravimetric data provided by field settling tube experiments to relate the median floc settling velocity ($Ws_{50}$) to the SPM concentration (Dyer, 1986). However, both of these parameterisation techniques do not include the important influential effects of turbulence.

More theoretically-based flocculation formulae have been offered (e.g. van Leussen, 1994; Argaman and Kaufman, 1970), but these are equations often containing many coefficients which are very difficult to calibrate. An approach which has recently gained much interest by modellers, is the fractal representation of flocs (e.g. Hill, 1996; Winterwerp, 1999), which is based on Krone's (1963) *order of aggregation*. However, in order to make a fractal-based model solvable analytically within a numerical sediment transport simulation, a mean fractal dimension is commonly assumed, which may not be truly representative.

Therefore, apart from the general fact that suspended particulate matter flocculates and flocculation typically dominates over break-up, to-date it has been difficult to accurately quantify the influence and occurrence of flocculation, as well as floc break-up, on in-situ estuarine floc distributions. This is mainly due to the fragility of observing the fastest settling macroflocs, which are easily broken-up upon sampling (Gibbs and Konwar, 1983).

The generality in application of existing floc parameterisation techniques specifically for mass settling flux determination, is a point of extreme debate and conjecture. It is therefore the aim of this paper to describe a new flocculation model, referred to as the Manning Floc Settling Velocity (MFSV) model, which was developed as part of the UK Defra funded Estuary Processes research project — EstProc (HR Wallingford, 2002). The MFSV was based entirely on experimental observations made using low intrusive video data acquisition techniques, from a wide range of estuarine water column conditions. The Manning empirical model will be used to reveal the principle inter-relationships controlling natural mud flocculation, and how this consequently affects the resultant mass settling fluxes. The MFSV algorithms will then be assessed and compared against observed data, followed by other approaches which are often incorporated in numerical sediment transport simulation models to parameterise the vertical mass flux.

## 2. Data sources and acquisition

The data utilised in this study were acquired predominantly from a series of in-situ experiments conducted in several European estuaries. Sampling deployments were conducted on a sub-tidal cycle time scale at periods when the flow conditions were either reasonably steady or gradually changing. Flocs were sampled using the low intrusive, video-based INSSEV : IN-Situ SEttling Velocity instrument (Fennessy et al., 1994a; Manning and Dyer, 2002a), as illustrated in Fig. 1. High frequency flow velocity and SPM concentration time series data were recorded at 18 Hz using four two-channel 2 cm diameter discoidal electro-magnetic current meters (EMCM) and eight optical backscatter sensors (OBS), respectively. EMCM and OBS calibrations are described by Christie et al. (1997) and Dyer et al. (2004). These sensors were laterally off-set from the INSSEV sampling unit. Vertical profiles of temperature and salinity were also taken at regular intervals.

The majority of the floc sampling was made in the Tamar estuary (UK) as part of the European Commission MAST III funded COSINUS project (Berlamont, 2002). A series of four experiments provided a total of 91 floc

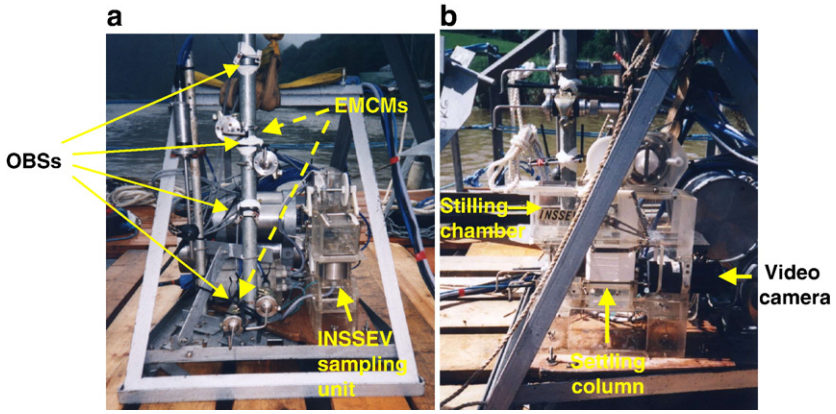


Fig. 1. INSSEV and POST sensors mounted on the estuarine bed frame — (a) front view and (b) side view.

populations (i.e. complete spectral samples) which were measured during neap and spring tidal conditions (Dyer et al., 2002a; Manning and Dyer, 2002b). The Tamar is classified as a mesotidal estuary at neap tides, and macrotidal during spring conditions, with respective average tidal ranges of 2.2 m and 4.7 m. The measurements were conducted in the head region of the estuary near Calstock (which is about 30 km from the mouth) in a straight reach of the estuary within the tidal trajectory of the turbidity maximum. Throughout the entire COSINUS experimental series turbulent shear stresses ($\tau$) and SPM concentrations, at the INSSEV sampling height, ranged from 0.04-0.7 N $m^{-2}$ and 0.01–8.6 g $l^{-1}$, respectively. Of particular note was the observation of a concentrated benthic suspension (CBS) layer forming in the near-bed region at mid-tide periods during spring conditions. This created drag reduction at the lutocline and turbulence damping within the CBS layer, and had a net influence on enhancing the flocculation process. These aspects are further discussed by Dyer et al. (2002b, 2004).

Additional floc samples were obtained from deployments conducted in the Gironde estuary (south-west France), which is 140 km in length, macrotidal and predominantly well mixed. These 34 floc measurements (Manning et al., 2004), acquired during the EC TMR SWAMIEE project (Manning et al., 2001), experienced neap tidal conditions where the tidal range in the lower reaches of the Gironde estuary, near Le Verdon, was about 2 m. Together the Rivers Garonne and Dordogne produce an annually-averaged river discharge of 760 $m^3$ $s^{-1}$. Although at times peak shear stresses reached 1.94 N $m^{-2}$, SPM concentrations did not exceed 600 mg $l^{-1}$.

Within the framework of the EC MAST III INTRMUD project (Dyer et al., 2000), 11 measurements were made during neap tides in the mesotidal Dollard estuary. It is a well mixed embayment fringing the southern part of the Ems estuary. It is located in the north-eastern part of the Dutch Wadden Sea on the border with Germany. In contrast to the Tamar and Gironde in-situ experiments, the instrumentation was deployed on inter-tidal mudflats, where the high water depth was 1.5 m. The Dollard comprises a surface area of 112 $km^2$ (76 $km^2$ are the inter-tidal flats) of the total 500 $km^2$ Ems system. The main freshwater input comes from the Ems River which has an annual mean discharge of 20 $m^3$ $s^{-1}$, although seasonally this can vary from 25 $m^3$ $s^{-1}$ to 390 $m^3$ $s^{-1}$. Again in contrast to the Tamar and Gironde, the Dollard is an ebb dominant estuary. Particle entrainment and turbulence levels were similar to those observed during neap tides in the Tamar estuary. The Dollard estuary floc characteristics are reported by Manning (2004b). Supplementary flocculation data was provided from a series of controlled hydraulic laboratory simulations (Gratiot and Manning, 2004) conducted at the Laboratoire des Ecoulements Geophysiques et Industriels (LEGI) in Grenoble, France.

## 3. Data processing

### 3.1. Floc data

For each floc population observed by INSSEV individual spherical equivalent floc diameters ($D$) and floc settling velocities were measured. The simultaneous measurement of $D$ and Ws allowed the effective density ($\rho_e$) of individual flocs to be calculated from a re-arranged Stokes' Law relationship. Computational techniques derived by Fennessy et al. (1997), were then applied to calculate individual floc dry mass and the mass settling flux (MSF) distribution for each INSSEV floc sample. Further details on the floc data processing are provided by Manning (2004b).

The mean size is the most commonly used floc parameter. However, from a quantitative perspective, the large variations in floc density, size and settling velocity which are often apparent in any one sample tend to question the validity of a single mean value. A conclusion drawn from an Inter-comparison Experiment of various floc measuring devices conducted in the Elbe estuary (Dyer et al., 1996), was that a more accurate representation of floc population settling characteristics could be achieved by splitting a distribution into two or more floc size fractions, each with their own mean settling velocity. Both Eisma (1986) and Manning (2001) recommend the use of a macrofloc and microfloc categorisation, and this segregation was adopted for this study.

An initial statistical appraisal of the data reported in this study, revealed that 160 μm provided the optimum separation point between the macrofloc and microfloc fractions, in particular in terms of the settling velocity and dry mass of each floc sub-population for a wide range of $\tau$ and SPM conditions. Both macrofloc ($D$>160 μm) and microfloc ($D$<160 μm) properties were calculated for each floc sample.

### 3.2. Turbulence data

The three orthogonal components of flow measured by the EMCMs enabled the turbulent shear stresses to be quantified from the turbulent kinetic energy (TKE) derived using the following relationship (e.g. Stapleton and Huntley, 1995):

$$\mathrm{TKE} = 0.5\rho_W\left(\overline{u'^2} + \overline{v'^2} + \overline{w'^2}\right) \quad (1)$$

where $\overline{u'^2}$, $\overline{v'^2}$ and $\overline{w'^2}$ are the variances of the three turbulent fluctuating components calculated from each 4096 data point file (at 18 Hz). By assuming the energy production equals the energy dissipation (Nakagawa and Nezu, 1975), the turbulent shear stress ($\tau$) can be calculated from TKE by applying Soulsby's (1983) constant of proportionality.

### 3.3. Multiple regression analysis

A parametric multiple regression technique was chosen to analyse the empirical data matrix and generate statistical relationships from the experimental data. The statistical package Minitab for Windows — version 10.1 was used for all the regression analysis, with a default statistical confidence level of 95%. The aim was to separate the field of varying SPM concentration and $\tau$ empirical results, by curves representative of a number of parameter ranges. The following floc characteristics were considered the most important and relevant for the analysis (abbreviations used in brackets):

- Macrofloc settling velocity ($Ws_{macro}$)
- Microfloc settling velocity ($Ws_{micro}$)
- Percentage of SPM constituting the macrofloc portion of a floc population ($SPM\%_{macro}$)
- Percentage of SPM constituting the microfloc portion of a floc population ($SPM\%_{micro}$)
- Total SPM concentration (SPM)
- A turbulence parameter ($\tau$).

The division of particulate matter within a floc population, and the relative rates at which they settle, are the key variables which govern the deposition of the matter in suspension; i.e. the mass settling flux, and these are represented by the first five terms. Also the physical descriptors of SPM concentration and a turbulence parameter, represent the basic factors which govern the collision rate and subsequent degree of flocculation of particles in estuarine waters. In this quantitative study, salinity was not regarded as a prime factor in flocculation, as significant levels of flocculation were observed in the Tamar and Dollard when the water was predominantly fresh. Also, organic matter descriptors were omitted from the analysis, as there were only a limited number of biochemical samples available, and the EstProc remit required a primarily physical floc settling model.

For consistency, the following units were used for each parameter included in the multiple regression and comparison analysis: $\tau$=N m$^{-2}$, SPM=mg l$^{-1}$, Ws=mm s$^{-1}$, $D$=μm, and $SPM\%_{macro}$ and $SPM\%_{micro}$=both expressed as a percentage.

## 4. Results

The regression analysis which produced the MFSV empirical model (denoted by the suffix EM) for estuarine flocculation was based on a combined data matrix consisting of 157 individually observed floc populations. The derived algorithms are valid for SPM concentration and $\tau$ values ranging between 10 and 8600 mg l$^{-1}$ and 0.04 and 2.13 N m$^{-2}$ (with extrapolation extending this up to 10 N m$^{-2}$), respectively. The Manning empirical model was composed of three principle component algorithms: $Ws_{macroEM}$, $Ws_{microEM}$ and $SPM_{ratioEM}$; each will be discussed in turn.

### 4.1. Macrofloc settling velocity ($Ws_{macroEM}$)

Macroflocs ($D$>160 μm) are recognised as the most important sub-group of flocs, as their fast settling velocities

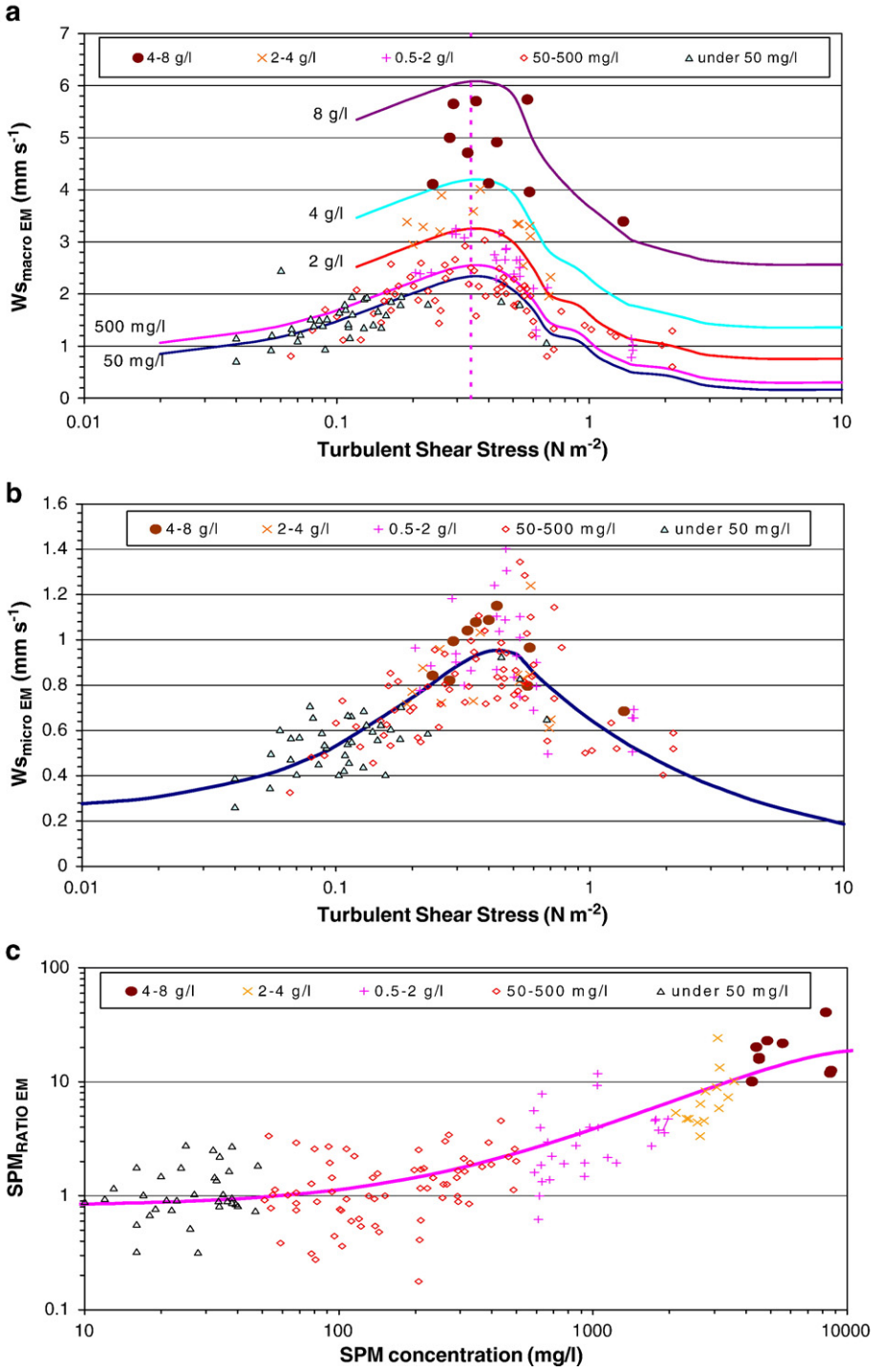


Fig. 2. Representative plots of the statistically generated regression curves, together with the experimental data points, illustrating the three contributing components for the empirical flocculation model: a) $Ws_{macroEM}$ (Eqs. (2a), (2b), and (2c)) at various constant SPM values plotted against $\tau$, vertical dotted line illustrates $\tau = 0.34$ N m$^{-2}$; b) $Ws_{microEM}$ (Eqs. (3a) and (3b)) plotted against $\tau$; and c) $SPM_{ratioEM}$ (Eq. (4)) plotted against SPM concentration.

tend to have the most influence on the mass settling flux. Their fragile, low density structure makes them very sensitive to physical disruption during sampling. Consequently, most previous experimental studies have tended to emphasise and favour the smaller microflocs. Although it is quite feasible that some fragile macroflocs may be transported through the water column by advection, on arriving at the INSSEV sampling location they would attain an equilibrium with the local shear stress conditions very quickly, in accordance with the theoretical flocculation time constraints.

The multiple regression revealed that the $Ws_{macroEM}$ showed a dependency on both $\tau$ and SPM concentration variations. It was not possible for a single equation to encompass the entire experimental range of turbulent shear stress, and thus the data was split into three $\tau$ zones which could be joined at their adjacent boundaries.

For $\tau$ ranging between 0.04 and 0.65 N $m^{-2}$:

$$Ws_{macroEM} = 0.644 = 0.000471\ SPM + 9.36\tau - 13.1\tau^2 \quad R^2 = 0.93 \tag{2a}$$

For $\tau$ ranging between 0.65 and 1.45 N $m^{-2}$:

$$Ws_{macroEM} = 3.96 + 0.000346\ SPM - 4.38\tau + 1.33\tau^2 \quad R^2 = 0.90 \tag{2b}$$

For $\tau$ ranging between 1.45 and 5 N $m^{-2}$:

$$Ws_{macroEM} = 1.18 + 0.000302\ SPM - 0.491\tau + 0.057\tau^2 \quad R^2 = 0.99. \tag{2c}$$

Each formulation is valid for concentration values of about 10–20 mg $l^{-1}$ up to 8.5 g $l^{-1}$. Statistical analysis showed that higher orders of SPM and $\tau$ did not significantly improve the algorithm accuracy. Continuity between each relationship can be achieved by calculating a $Ws_{macro}$ value using both adjacent equations (at a specific $\tau$) and obtaining a single transitional $Ws_{macro}$ value from linear interpolation. However, no data points were available for SPM concentrations over 1 g $l^{-1}$ when the turbulent shear stress fell below 0.1 N $m^{-2}$, and therefore this should be regarded as a further boundary limit to Eq. (2a). The regression analysis indicated that the concentration contributed 66% of the total variance, whilst the remaining 34% was attributed to the turbulence parameters. When considering the latter in detail, approximately a third of the 34% turbulence variance (i.e. about 12% of the total variance) is accredited to the $\tau^2$ term.

The complete regression curves described by Eqs. (2a) (2b) (2c) are represented graphically in Fig. 2a. Generally, $Ws_{macroEM}$ displays a similar trend to the conceptual relationship originally proposed by Dyer (1989), and recently reported by Winterwerp et al. (2006), with an increase in settling velocity at low shear stresses due to flocculation enhanced by shear, and a decrease in settling velocity due to floc disruption at higher stresses for the same concentration. The fastest $Ws_{macroEM}$ values occurred at a turbulent shear stress of about 0.36 N $m^{-2}$. This shear stress threshold corresponds very closely to the value observed during a series of laboratory annular flume experiments by Manning and Dyer (1999).

The peak macrofloc settling velocities (~4–6 mm $s^{-1}$) were representative of flocs which form within a CBS layer, where damping effects reduce the magnitude of the turbulent stirring. At this point the collision frequency appeared to be at its optimum for flocculation and stimulated the growth of fast settling macroflocs. Beyond 0.4 N $m^{-2}$, the regression shows the $Ws_{macroEM}$ values decreased rapidly in response to disaggregation as the turbulent shear increased. For a sheared suspension of 4 g $l^{-1}$, a $\tau$ of 0.7 N $m^{-2}$ led to a 33% decrease in $Ws_{macroEM}$. This must be the effect of the continued increase in shear creating more destructive collisions between the abundant macroflocs, and negating contacts which may promote flocculation. The decrease in settling velocity would therefore be attributed to a general reduction in the floc size range within the macrofloc sub-group.

Above a stress of 1.4 N $m^{-2}$, the $Ws_{macroEM}$ tended to decrease more slowly with increasing shear. One could hypothesise that beyond 1 N $m^{-2}$, only a limited number of very resilient macroflocs would exist, and further growth would be eradicated with a continued rise in shear stress. This small number of very strong macroflocs would have been created during highly turbulent events, and retained that "history". For applied modelling purposes, above a $\tau$ of about 5 N $m^{-2}$, the $Ws_{macroEM}$ can be considered to remain effectively constant.

### 4.2. Microflocs settling velocity ($Ws_{microEM}$)

The smaller microflocs ($D$<160 μm) are generally considered to be the building blocks from which the macroflocs are composed. Field studies by McCave (1975), Alldredge and Gotschalk (1988), Fennessy et al. (1994b), and Manning (2001) all show the microfloc class of aggregate tends to display a much wider range in effective densities and settling velocities than the larger floc fraction. The settling trends of the microflocs were represented by two sub-algorithms.

Table 1
Summary of floc parameterisation approaches used during the testing of the Manning empirical flocculation algorithms

| Method number | Description |
|---|---|
| M1 | Manning empirical Flocculation model (Eq. (5)) |
| M2 | Constant setting velocity, Ws=0.5 mm $s^{-1}$ |
| M3 | Constant setting velocity, Ws=0.5 mm $s^{-1}$ |
| M4 | $Ws_{mean}$–SPM concentration power regression relationship (Eq. (6)) |
| M5 | van Leussen (1994) approach (Eq. (7)) |

For $\tau$ ranging between 0.04 and 0.52 N $m^{-2}$:

$$Ws_{microEM} = 0.244 + 3.25\tau - 3.71\tau^2 \quad R^2 = 0.75 \quad (3a)$$

For $\tau$ ranging between 0.52 and 10 N $m^{-2}$:

$$Ws_{microEM} = 0.65\tau^{-0.541} \quad R^2 = 0.73. \quad (3b)$$

The most prominent difference to be revealed from the regression when comparing the $Ws_{macroEM}$ and $Ws_{microEM}$ algorithms was the negligible influence of SPM concentration variations on the latter. This is most likely due to the microflocs being the building blocks from which the macroflocs are formed from. The shape of the regression curve is illustrated graphically in Fig. 2b, where it is plotted together with the corresponding data points.

$Ws_{microEM}$ demonstrated a correlation solely with turbulent shear stress. The lower $R^2$ values of algorithms (3a) and (3b), when compared to those of the macrofloc settling velocity, was partly a result of the greater variability in the individual settling velocities and effective densities exhibited by the microfloc distributions, from which each of the average microfloc settling velocities was calculated. The scatter is a reflection of the greater variability in the settling and compositional properties exhibited by individual microflocs within a single floc population. This in turn would have an effect on each $Ws_{microEM}$ value calculated, however an $R^2$ of 0.73–0.75 suggests that the scatter is relatively small. Hence, these equations are deemed representative of the empirical data, for modelling applications.

As with the macroflocs, the microfloc settling velocity rose with increasing shear stress until a peak $Ws_{microEM}$ of ~1 mm $s^{-1}$ was reached at a limiting $\tau$ of ~0.44 N $m^{-2}$. This could be the result of the breaking of macroflocs, which attained their peak velocity at a much lower critical shear stress. Most of these faster settling microflocs were between 120 and 160 μm in diameter. The higher limiting shear stress for the microflocs can probably be attributed to their stronger inter-connective bonds, which Eisma (1986) attributes to biogenic "glues" produced by organisms, such as extracellular polymeric substances (Tolhurst et al., 2002), together with their residence time history.

### 4.3. SPM ratio ($SPM_{ratioEM}$)

To categorise the distribution of particulate matter throughout the macrofloc and microfloc sub-populations, the dimensionless SPM ratio (Manning, 2004b) is used. This was calculated by dividing the percentage of $SPM_{macro}$ by the percentage of $SPM_{micro}$ (both by mass concentration) for each floc population. It must be stressed that this type of computation is unique to instruments such as INSSEV or LabSFLOC (Manning et al., 2006), which can accurately and reliably estimate the floc effective density (by simultaneous size and settling velocity observations) of each individual floc from a respective population. Without this type of measurement, it is not possible to apportion the SPM concentration with any confidence between the microfloc and macrofloc groups.

In contrast to the $Ws_{microEM}$, the $SPM_{ratioEM}$ (SPM units of mg $l^{-1}$) showed a strong dependency solely with SPM concentration (Fig. 2c).

$$SPM_{ratioEM} = 0.815 + 3.18 \times 10^{-3}\ SPM - 1.4 \times 10^{-7}\ SPM^2 \quad R^2 = 0.73. \quad (4)$$

Low concentrations (10–100 mg $l^{-1}$), such as those typically observed on an ebb during neap tides in the flood dominant Tamar estuary, tended to create an equally balanced floc population with an $SPM_{ratioEM}$ of approximately unity. Whereas the periods of high entrainment encountered during the more dynamic spring tides, could see the $SPM_{ratioEM}$ rise to between 10 and 20 for SPM concentrations>4 g $l^{-1}$. This corresponds to 91–95.3% of the particulate mass in suspension being contained by macroflocs. This would have a significant effect on the dynamics of a settling floc population and inevitably on the depositional flux.

### 4.4. Mass settling flux ($MSF_{EM}$)

The MFSV Eqs. (2a), (2b), (2c), (3a), (3b) and (4) can be combined to form Eq. (5) from which the total mass settling flux, $MSF_{EM}$ (with the units of mg $m^{-2}s^{-1}$), can be calculated:

$$MSF_{EM} = \left[\left(1 - \frac{1}{1 + SPM_{ratioEM}}\right) \cdot (SPM \cdot Ws_{macroEM})\right] + \left[\frac{1}{1 + SPM_{ratioEM}} \cdot (SPM \cdot Ws_{microEM})\right]. \quad (5)$$

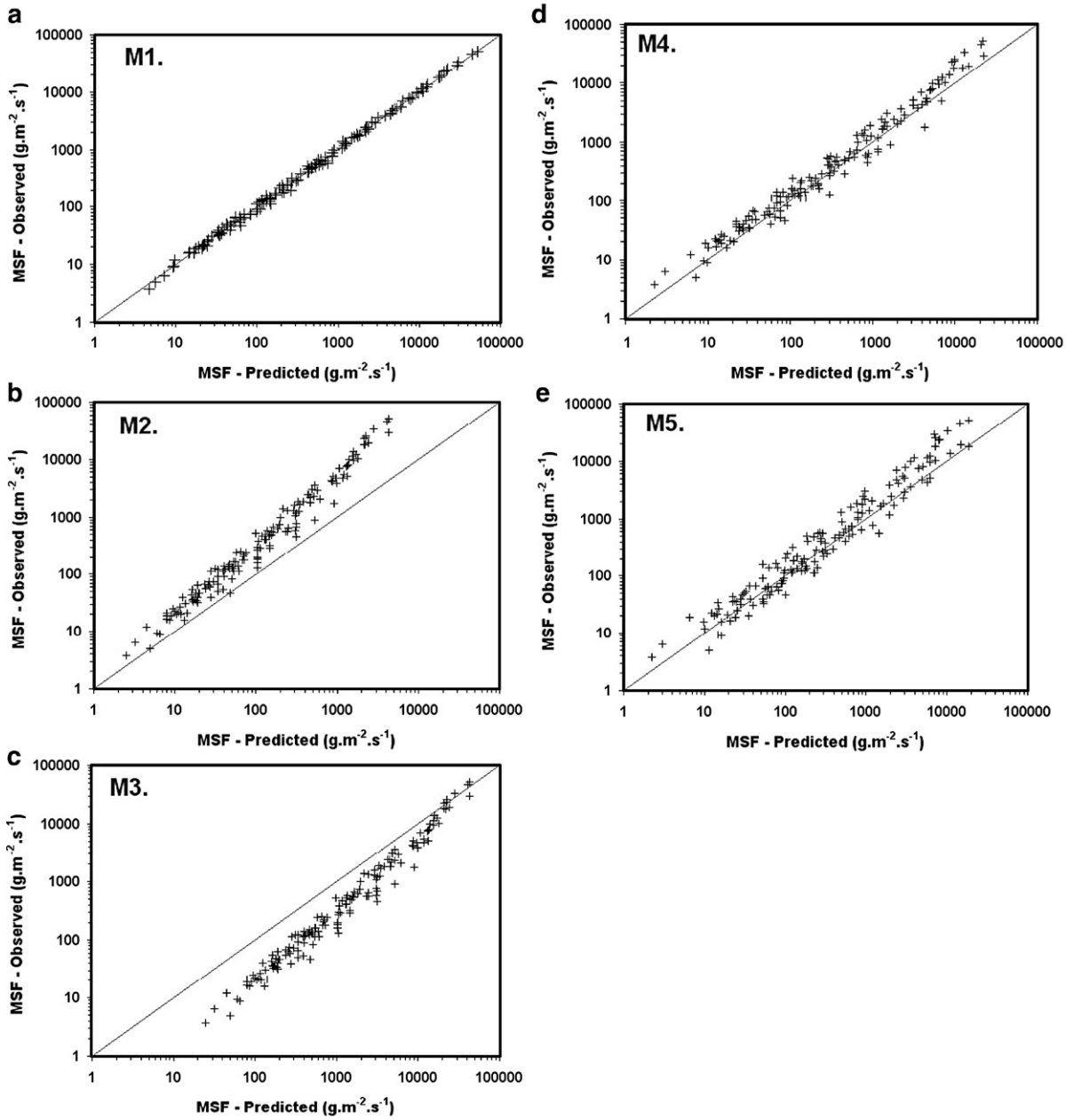


Fig. 3. The 157 individual mass setting flux (MSF) observations plotted against the corresponding 157 MSF values as predicted by each floc model approach (M1–M5).

This is a very practical way of expressing the inter-relationship between the three core algorithms and can easily be implemented in mathematical simulation models. Within a sediment transport model framework, each value of $MSF_{EM}$ calculated for a specific point in the water column, can be linked to the depositional flux by either the conventional depositional shear stress threshold, or the depositional approach advocated by Winterwerp (2006).

A comparison of the three $R^2$ statistical fit values indicates that the macrofloc settling velocity is the more consistently predictable parameter, with $R^2$ values generally exceeding 0.9. The $R^2$ values of 0.73–0.75 for the remaining two parameters still means that these representations are highly significant for natural empirical data regressed at a confidence level of 95%.

## 5. Assessment of empirical model

In order to quantify the accuracy of the MFSV model, it was tested and compared with a number of existing approaches to parameterise floc settling. This comparison uses both the original data set from which the MFSV algorithms are derived (Section 5.2), to provide a sense of relative representation accuracy, and then an independent data set is also employed (Section 5.3) as a second stage assessment. Numerical models are used to simulate deposition rates, not settling velocities, so this inter-comparison will be in the form of a prediction of mass settling flux. This requires a MSF value to be calculated for each entire floc spectrum. Once a modelling approach is formulated and calibrated (where necessary), the only parameters which will be available for each model to calculate a MSF rate will be an input of a $\tau$ and SPM concentration value. This is very similar to how a fully 3-D numerical model would utilise a flocculation algorithm, and hence this provides a realistic and equal test of each method's predictive performance.

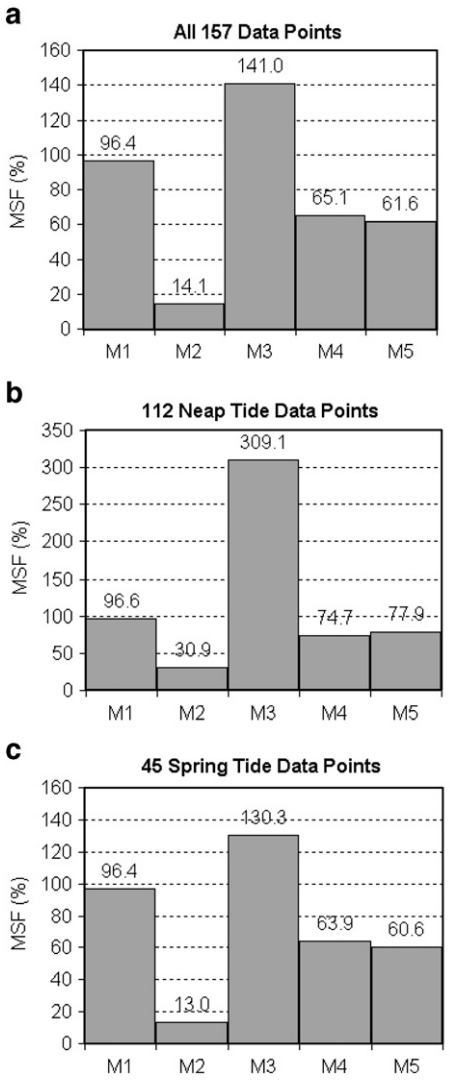


Fig. 4. The cumulative total mass setting flux (MSF) expressed as percentage, as calculated by each modelling method, for a) all 157 flux values, b) neap tides (112 flux values), and c) spring tides (45 flux values). 100%=total observed MSF.

### 5.1. Comparison methods used

A total of five methods (denoted by *M*) were employed in the comparison with the original data set (a summary is provided in Table 1), and each parameterisation technique will be outlined in turn. The first (M1) are the MFSV algorithms in the form of Eq. (5). The next two methods (M2–M3) employed single constant values of floc settling velocity. This is a very common approach used in numerical modelling, as it requires the least amount of programming code, and thus reduces a model's processing time. A single settling value says very little about the floc characteristics or how they change throughout a tidal cycle. The settling velocity values employed span commonly quoted values: M2, 0.5 mm $s^{-1}$ and M3, 5 mm $s^{-1}$. The slowest of these settling velocities is generally representative of mean settling rates determined by gravimetric analysis of field settling tube data, whereas the faster settling rate is a value which has been included in a recent simulation model of the Tamar estuary by Petersen et al. (2002).

M4 uses an exponential power regression relationship between the mean settling velocity and ($Ws_{spm}$) the SPM concentration (Eq. (6))

$$Ws_{spm} = 0.36\ SPM^{0.234}. \quad (6)$$

The fifth comparative method (M5) utilised the formulation advocated by van Leussen (1994). The $Ws_{VL}$ algorithm form is shown in Eq. (7), where *G* is a turbulence parameter:

$$Ws_{VL} = Ws_{Ref}\ \frac{1 + a\,G}{1 + b\,G^2}. \quad (7)$$

In order to be consistent in the calibration of the coefficients for these latter two expressions Eqs. (6) and (7), the data set from which the Manning settling model was originally derived was used. The best fit (albeit quite poor) to the data matrix was achieved with the constants $a=0.3$ and $b=0.05$. The coefficients were similar to values obtained by Roberts (pers. Comm, 1999) for the Tamar estuary. The reference settling velocity component ($Ws_{Ref}$) requires the mean settling

rate to be expressed in terms of SPM concentration by a power regression. For this purpose, Eq. (6) was used.

### 5.2. Comparison with original empirical data

Fig. 3 shows the individual MSF values predicted by each of the five modelling approaches plotted against the corresponding measured (i.e. observed) MSF rates for each of the 157 cases. A statistical assessment was conducted to quantify the deviation of the 157 values calculated by each predictive method, from the 1 to 1 exact-fit line plotted on Fig. 3a–e. First a mean error (expressed as a percentage) was calculated for each floc model, to indicate how much each predicted point typically deviates from the measured value for all 157 fluxes. The degree of dispersion about the mean is indicated by the corresponding standard deviations.

A comparison of each pair of individual settling flux values (i.e. predicted and observed) provides only a limited assessment of a model's predictive qualities, as it assumes an equal weighting for each of the 157 observations. However, the complete data set comprised fluxes measured throughout a wide range of estuarine conditions. Also, when modelling the movement of estuarine sediments throughout consecutive tidal cycles, the precise estimation of the largest fluxes is crucial. Therefore a comparison was made between the measured cumulative total mass settling flux (i.e. the summation of all the 157 individual flux values), which totalled 496 g $m^{-2}$ $s^{-1}$, and the corresponding cumulative flux totals estimated by each of the five algorithms. The difference in over- or under-prediction by each method, relative to the measured flux total, is expressed as a percentage and illustrated in Fig. 4. All the statistical results are summarised in Table 2.

The MSF values calculated by the MFSV showed a very close fit to the 45° line throughout the entire range of turbulence and concentration conditions (Fig. 3a). Statistically, each individual settling flux estimated by MFSV was in mean error by only 0.8%, at a standard deviation of 10.3% about the mean. This translated into a 96.4% estimation of the cumulative total mass settling flux for all 157 (Fig. 4a). The constant settling rates produced a 126% variation in total settling flux, with under-predictions of 85% for the slowest velocity (M2), through to 41% over-predictions for a constant 5 mm $s^{-1}$. From an initial assessment, methods M4 and M5 seemed to have all performed reasonably well, by producing mean errors of about 15%. However, the significant amount of scatter around the 45° line (Fig. 3d–e) was reflected in standard deviations 3–4 times greater than those obtained for MFSV. In terms of the cumulative total flux, the last two approaches only predicted between 61 and 65% of the flux. Reasons for the wide dispersion in the flux values calculated by methods M4 and M5 will be discussed later in this paper.

To gain a greater insight into how each model performed during different tidal conditions, comparisons were made by separating the 157 floc data matrix into the neap and spring tidal sub-components. The 112 cases representative of neap tides produced a cumulative total MSF of 28,663 mg $m^{-2}$ $s^{-1}$, and the MFSV estimate was within 3.4% of this total (Fig. 4b). Fig. 5a shows the scatter of the individual neap tide model predicted flux values relative to the measured fluxes (which are equal to 100%), all plotted against SPM concentration. MFSV showed little deviation from the 100% mark, with some individual estimates being in error by an average of only 0.3%.

The low level of suspended concentration, which was typically under 700 mg $l^{-1}$ for neap conditions, resulted in a 25.3% under-estimate in the cumulative total MSF by the SPM power regression (M4) approach. The inclusion of the turbulence parameter as implemented by the van Leussen (1994) method (M5) did not fare much better, with a predicted MSF total of 77.9% when compared to the observations. The very simplified

Table 2
Summary of the statistical output from each of the five approaches mass settling flux predictions in comparison to the observed values

| | Statistical test | M1 | M2 | M3 | M4 | M5 |
|---|---|---|---|---|---|---|
| All 157 floc samples | Mean error (%) | −0.8 | −64.5 | 255.4 | −15.4 | 15.7 |
| | Standard deviation | 10.3 | 17.9 | 178.7 | 34.4 | 31.8 |
| | Total cumulative MSF (%) | 96.4 | 14.1 | 141.0 | 65.1 | 61.6 |
| 112 Neap tide floc samples | Mean error (%) | −0.3 | −58.1 | 319.2 | −14.0 | −111.5 |
| | Standard deviation | 11.5 | 16.2 | 162.1 | 34.1 | 33.4 |
| | Total cumulative MSF (%) | 96.6 | 30.9 | 309.1 | 74.7 | 77.9 |
| 45 Spring tide floc samples | Mean error (%) | −1.9 | −80.4 | 96.5 | −18.7 | −25.9 |
| | Standard deviation | 6.4 | 10.4 | 103.6 | 35.5 | 24.6 |
| | Total cumulative MSF (%) | 96.4 | 13.0 | 130.3 | 63.9 | 60.6 |

Negative mean error values indicate under-estimates. The observed total cumulative MSF = 100%.

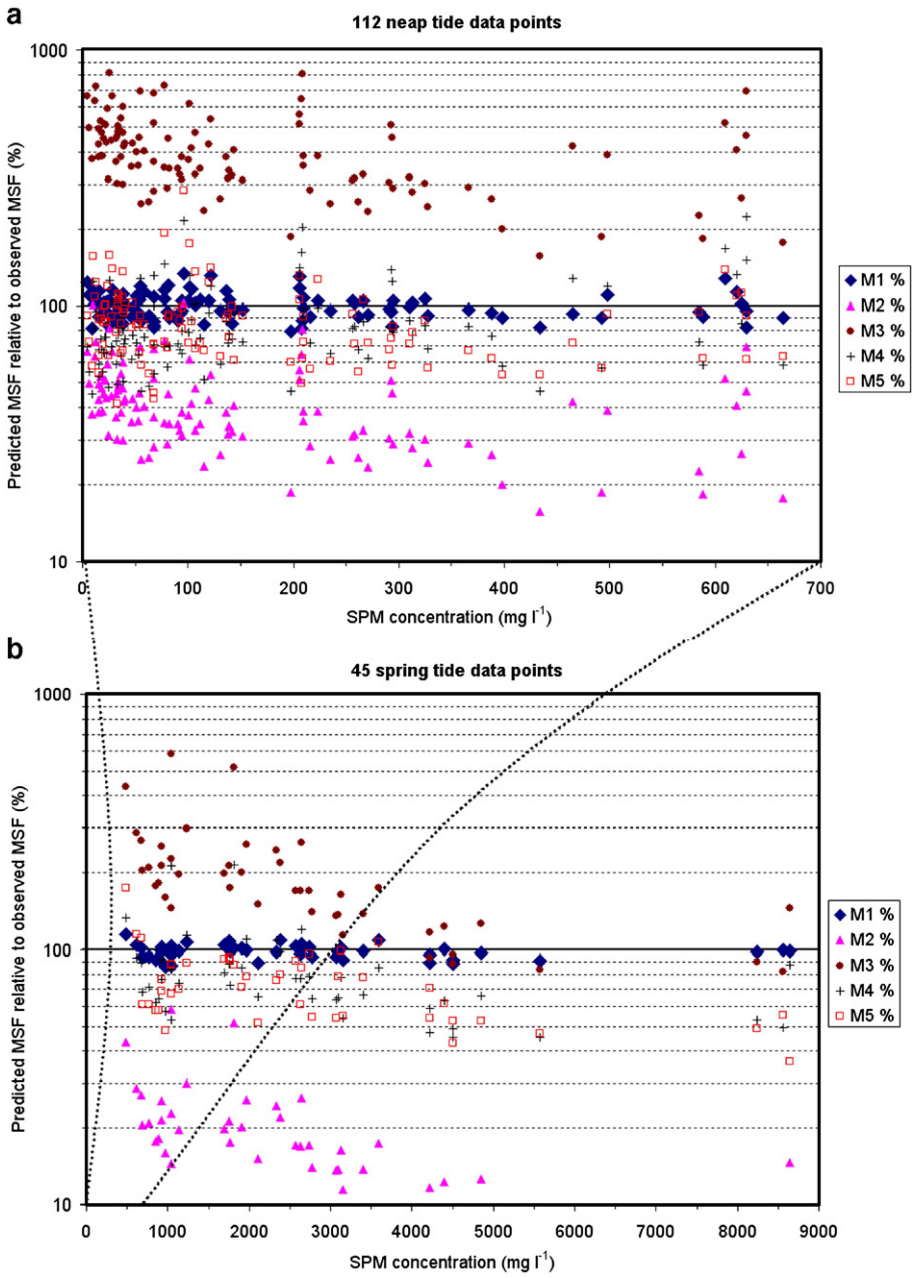


Fig. 5. Individual mass setting flux (MSF) values, as predicted by each floc model approach (M1–M5) plotted against SPM concentrations; for a) 112 neap tide data points and b) 45 spring tide data points. Each corresponding observed flux value is equal to 100%.

constant settling velocities provided a wide range of errors depending upon the value chosen. The 0.5 mm $s^{-1}$ is representative of what could be classified as typical microfloc settling velocities, and under-predicted the total neaps flux by 69.1%. Whereas, the 209.1% over-estimate by M3 (a constant 5 mm $s^{-1}$) shows that just assigning a faster settling velocity, would produce an even greater misrepresentation of the settling flux. At times method M3 produced individual flux over-predictions of up to 700% (Fig. 5a). Generally, the mean error in individual mass flux predictions, and the degree in their dispersion, increased with each faster constant settling velocity.

The significant increase in SPM concentration (>700 mg $l^{-1}$) during spring tide conditions did not greatly affect the MSF prediction of method MFSV, which calculated a cumulative total springs MSF of 450 g $m^{-2}$ $s^{-1}$; this was still only 4.6% less than the

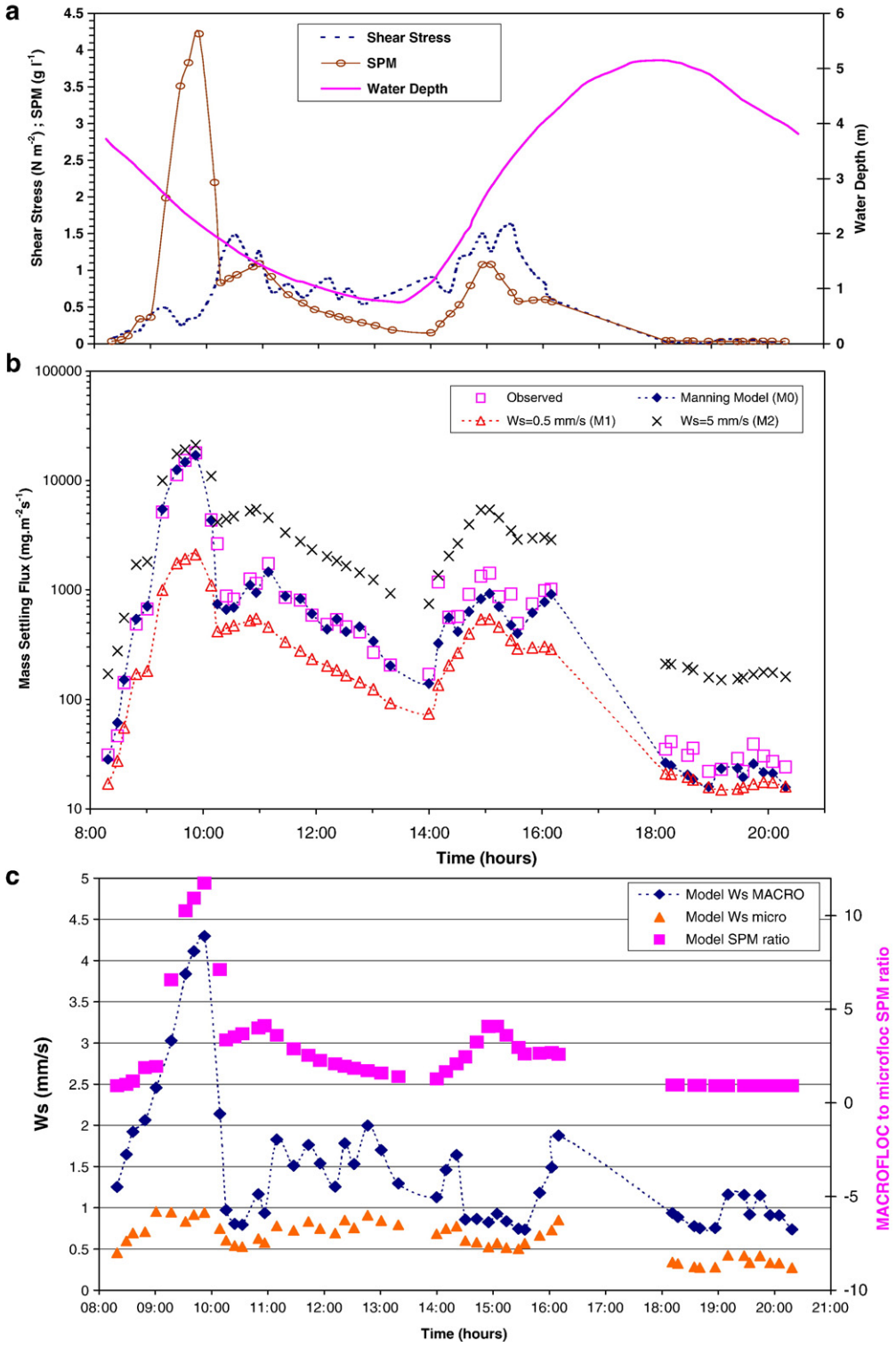


Fig. 6. a) Time series of upper Tamar estuary variables ($\tau$ and SPM at 0.5 m above bed) acquired on 15th April 2005, b) observed and predicted mass setting flux time series, c) MFSV component algorithm outputs for the tidal cycle.

measured flux rate (Fig. 4c). Apart from method M3, which still over-predicted by nearly 31%, the remaining methods all under-estimated the cumulative total flux by 36–87% (Fig. 4c). This was reflected in the greater degree of scatter demonstrated by the individual settling flux under-estimates of methods M2, M4 and M5 during the high concentration spring tides (Fig. 5b). In terms of their applicability to numerical sediment transport modelling, these excessive over- or under-predictions would minimise or even negate the significant influence of events where flocculation is a major contributor during a tidal cycle, especially within an estuarine turbidity maximum zone.

### 5.3. Comparison with independent empirical data

This comparison allows the MFSV model to be assessed with independently acquired MSF data. The independent data set comprises a complete tidal cycle of observations during spring tides in the Tamar estuary collected on 15th April 2003 (Bass et al., 2006; see Fig. 6a). During the mid-ebb, the surface flow attained a velocity of about 0.8 m $s^{-1}$. This coincided with a maximum turbulent shear stress of ~1.5 N $m^{-2}$. SPM concentration rose in response to the accelerating flow, and during the passage of the turbidity maximum reached a maximum concentration of 4.2 g $l^{-1}$ 4 h before low water. The stronger flood produced a peak surface flow velocity, approximately double the peak velocity observed during the ebb, just 1 h and 20 min after the turning of the tide. The maximum $\tau$ on the flood exceeded the peak ebb shear stress by 0.15 N $m^{-2}$.

Fig. 6b illustrates how the mass settling flux, both measured and predicted (at a constant distance of 0.5 m above the estuary bed), varied through four orders of magnitude during the complete tidal cycle. A peak settling flux of 18 g $m^{-2}$ $s^{-1}$ occurred within the turbidity maximum during the ebb (09:50 h). The corresponding output from the three component MFSV model algorithms are shown in Fig. 6c. This very high flux was dominated by fast settling flocs; the $Ws_{macroEM}$ was estimated at 4.3 mm $s^{-1}$ and 0.94 mm $s^{-1}$ was the corresponding microfloc settling rate ($Ws_{microEM}$). At this point in the time series, it was an over-estimate of 8% for the observed macrofloc settling velocity, and 28% for the microflocs. However the Manning model under-estimated the total flux at maximum SPM by only 5.2%, due to apportioning of the relative settling velocities by the $SPM_{ratioEM}$.

A minimum $MSF_{EM}$ of 23 mg $m^{-2}$ $s^{-1}$ was estimated by the model just after high water slack (19:10 h), and this value was in general agreement with the observations (Fig. 6b). The main difference between the turbidity maximum and high water flux, was partly attributed to the significantly slower settling velocities of the flocs observed throughout the latter conditions. At slack water the $Ws_{macroEM}$ was more than four times slower than within the TM zone, and the $Ws_{microEM}$ was only 0.42 mm $s^{-1}$, which is a 55% reduction in velocity. Both settling velocity sub-components at slack water were under-estimated by about 10%.

The other factor which contributed to the production of two significantly different mass settling fluxes, was the distribution of the floc mass at each instance. At slack water the $SPM_{ratioEM}$ was estimated as unity, which would represent an equal apportioning of the floc mass between the two floc sub-populations. In reality the macroflocs represented 39% of the mass, a difference of 11%. Whereas the $SPM_{ratioEM}$ was 12 within the turbidity maximum zone, which equates to the macroflocs constituting 92.4% of the dry floc mass, and this was within a few percent of the observed.

The more well mixed, turbulent flood ($\tau \sim 1.6$ N $m^{-2}$) produced a settling flux of 915 mg $m^{-2}$ $s^{-1}$, 1 h and 45 min into the flood, which was an order of magnitude lower than the corresponding mid-ebb settling flux. The Manning model estimated only 52% of the observed MSF which was present. This is due to the observations indicating approximately 700 mg $m^{-2}$ $s^{-1}$ of the total flux being due to a faster settling microfloc fraction, which was a complete reversal in macro-microfloc settling dynamics from the less turbulent mid-ebb. Whereas, the MFSV model suggested the floc populations during this turbulent period were still composed of 55–80% macrofloc mass.

## 6. Discussion and conclusions

The concept behind the MFSV flocculation model is very different from approaches M2–M5, in that it was based entirely upon empirical data of complete floc distributions measured within a well described turbulent environment. Although the application of multiple settling velocities is not entirely new to numerical modelling, these are usually settling values which remain constant. The parameterisation was then taken a stage further in the MFSV empirical model by apportioning the SPM concentration between the macrofloc and microfloc fractions, and correlating this mass to the respective settling velocities of each fraction.

It is only possible to obtain an insight into the suspended particulate matter distribution patterns Eq. (4) by observing the full range of flocs which constitute an entire population, on a repeatable basis. This may be

regarded as restrictive due to the wide range of floc sampling techniques currently available (e.g. laser diffraction particle sizers), some of which are logistically far easier to use and deploy than video-based devices in estuarine locations. However, the results shown in this paper have illustrated how important the initial acquisition of complete floc spectral distribution data of both the particulate mass and settling rates are, if a reliably accurate floc parameterisation is to be developed.

It is acknowledged that INSSEV's video image resolution limits it to measuring flocs greater than 20 μm in size (although the majority of the mass tends to be held by the larger macroflocs), and INSSEV could only observe flocs in the near-bed region (although the new INSSEV_LF can now measure flocs throughout the water column). However, the general quality and robustness demonstrated by the MFSV empirical algorithms in these inter-comparisons, is partly a reflection of the good quality of INSSEV floc samples used to create the data base from which the algorithms are derived.

The van Leussen (1994) approach is based on theoretical aggregation concepts, but during the inter-comparison M5 showed large predictive errors and limited ranges of practical application in calculating MSF values. Therefore, in a predictive sense the MFSV empirical model is a significant step in improving sediment transport numerical simulations. Although these M1 algorithms do not encompass all possible avenues related to the flocculation process, it comprises the key catalysts which influence the settling flux of natural estuarine muds. The inclusion of additional terms, such as those of biological influences on flocculation, may further improve the generality of the model's predictions. However, making the algorithms more complex increases the computer coding and number of iterative calculations required, so a compromise between increasing the model complexity to achieve further accuracy, must be achieved. Additionally, these bio-chemical parameters are not routinely monitored, or even included in most standard sediment transport models. Generally, as the flocculation model becomes more complex, the greater the problem in obtaining good calibration data.

There are significant risks in using a static settling parameterisations. For example at typical Tamar estuary neap tide conditions, a constant settling velocity of 0.5 mm $s^{-1}$ (M2) consistently under-estimated the total MSF by about 60–70% (Fig. 5a), whereas a settling rate of 5 mm $s^{-1}$ (M3) gave typical over-estimates of 100–500%. Employing the same constant settling rates for a spring tide simulation, generally reduced the predictive accuracy of method M2 by a further 18%, whilst M3 showed a 179 % improvement in predicting MSF in the near-bed region. This was mainly attributed to the increased abundance of faster settling macroflocs present in CBS layers which can develop during spring tides. However M3 performed the worst of all five methods for spring tide (original data) samples which were measured above the lutocline (i.e. lower SPM concentration and high turbulence created by drag reduction), typically registering a MSF over-estimate of 210 % for those particular water column conditions.

For the independent data set, the MFSV showed a very close representation of the TM zone conditions flux, and estimated 92.3% of the total tidal cycle MSF. The MFSV algorithms were most in error during the lower concentration, well mixed, turbulent flood conditions which tended to favour the microflocs, where it predicted just over two thirds of the actual settling flux. A constant 0.5 mm $s^{-1}$ would have under-estimated the TM flux by −85% and was found to be least in error for the flood period, where it still only estimated a third of the observed settling flux. Whilst flux estimates from a fixed settling rate of 5 mm $s^{-1}$ rose to +271% for the flood. The higher concentrations of the TM best suited the 5 mm $s^{-1}$, but still produced over-predictions of 47%. Thus, simply increasing a fixed settling velocity does not necessarily improve MSF estimates throughout a tidal cycle in a meso- or macrotidal estuary. Importantly, the 0.5–6 mm $s^{-1}$ settling velocity range demonstrated by the $Ws_{microEM}$ and $Ws_{macroEM}$ algorithms, closely match the Ws variations identified by newly developed morphological models, which must be present to allow an estuary to maintain equilibrium over a neap-spring cycle (Prandle et al., 2005).

The inconsistencies in the SPM power law and van Leussen methods (M4 and M5) are probably a result of their poor representation of the concentration term within a shear field. Whilst the van Leussen (1994) approach is further complicated by its total reliance upon a power regression representation of the SPM concentration sub-component. By a process of selectively eliminating data series from the main 157 sample matrix, one can deduce that M5 was reasonably stable in application for the following limited range of SPM and turbulent shear stress conditions: 10–500 mg $l^{-1}$ and 0.06–0.24 N $m^{-2}$. Within those confines M5 under-predicted the total settling flux by 14%, however the individual flux predictions were quite widely dispersed at a standard deviation of 39%.

The MFSV parameterisation demonstrated flexibility in adapting to a wide range of estuarine environmental conditions, specifically for applied modelling purposes, by producing reliable mass settling flux predictions in both

quiescent waters and the rare occurrence of very turbulent events where $\tau$ reached 1–10 N $m^{-2}$. The MFSV derived mass flux values were also validated for both water columns of very low turbidity and highly saturated benthic suspension layers with SPM concentrations approaching 8.6 g $l^{-1}$. For example, when Baugh (2004) implemented the Manning settling algorithms in a TELEMAC-3D (EDF, 1998) numerical model of the Thames estuary (UK), the results showed that the Manning algorithm further increased the amount of vertical variation in the simulated suspended concentrations. It also better reproduced the lateral suspended concentration pattern observed during the flood tide. Spearman (2004) has found similar improvements using the MFSV parameterisation, when applying it to 3D modelling of inter-tidal mudflats, and further implementation testing of the MFSV algorithms is continuing and will be reported in due course.

As one would expect, the MFSV model is an accurate reflection of the flocculation data it is based on. However the low standard deviations and scatter demonstrated by the MFSV empirical model when applied to a wide range of estuarine environmental conditions, in comparison to existing settling flux parameterisations, is a testament to its overall reliability and robustness. This is corroborated by the independent data assessment. The multiple regression analysis revealed it was possible to accurately gain an insight into the particulate matter distributions, within floc sub-groupings, by using an optical video-based technique that can observe the macroflocs and microflocs which constitute an entire population. Although the specific values predicted by Eqs. (2a) (2b) (2c) (3a) (3b) (4) may not be universally applicable to every estuary, further testing of the algorithms against data from other European estuaries (e.g. Medway, Scheldt) illustrate that the general form of each equation is fully validated. The MFSV empirical model provides estuarine scientists and engineers an alternative way of both assessing and quantifying flocculation. Settling estimates from Eqs. (2a) (2b) (2c) (3a) (3b) (4) can be regarded as a first stage approximation for modelling applications. Simple tuning of the algorithm coefficients can increase and refine the accuracy of the predictions for a specific estuary.

## Acknowledgements

The preparation of this paper was primarily funded by HR Wallingford (UK), and the Defra/EA Joint Flood and Coastal Defence Research and Development Program in Fluvial, Estuarine and Coastal Processes: Estuary Process Research (EstProc) project (contract no. FD1905/CSA5966). Tamar estuary experimental programme was funded by the EC MAST program as part of contract MAS3-CT97-0082 COSINUS (Prediction of cohesive sediment transport and bed dynamics in estuaries and coastal zones with integrated numerical simulation models). The Gironde estuary experiments were funded by the EC TMR SWAMIEE (Sediment and water movement in industrialised estuarine environments) project under contract no. ERBFMRXCT970111. The Dollard estuary experimental program was funded by the EC MAST project INTRMUD (The Morphological Development of Intertidal Mudflats) under contract MAS3-CT95-0022. Additional funding by the Natural Environmental Research Council (NERC), contract no. NER/M/S/2002/00108, is also gratefully acknowledged.

## References

Alldredge, A.L., Gotschalk, C., 1988. In-situ settling behaviour of marine snow. Limnol. Oceanogr. 33, 339–351.

Argaman, Y., Kaufman, W.J., 1970. Turbulence and flocculation. J. Sanitary Eng., ASCE 96, 223–241.

Bass, S.J., Manning, A.J., Dyer, K.R., 2006. Preliminary findings from a study of the upper reaches of the Tamar Estuary, UK, throughout a complete tidal cycle: part I. Linking sediment and hydrodynamic cycles. In: Maa, J.P.-Y., Sanford, L.P., Schoellhamer, D.H. (Eds.), Coastal and Estuarine Fine Sediment Processes — Proc. in Marine Science, INTERCOH-2003. Elsevier, Amsterdam, pp. 1–14.

Baugh, J., 2004. Implementation of Manning algorithm for settling velocity to an estuarine numerical model. HR Wallingford Ltd (UK) Technical Report No. TR 146. 10p.

Berlamont, J.E., 2002. Prediction of cohesive sediment transport and bed dynamics in estuaries and coastal zones with integrated numerical simulation models. In: Winterwerp, J.C., Kranenburg, C. (Eds.), Fine Sediment Dynamics in the Marine Environment — Proc. in Mar. Sci. 5. Elsevier, Amsterdam, pp. 1–4.

Christie, M.C., Quartley, C.P., Dyer, K.R., 1997. The development of the POST system for in-situ intertidal measurements. Proc. 7th Int. Conf. On Elec. Eng. in Oceanography, Conference Publication No. 439, Inst. Elec. Eng., London, pp. 39–45.

Dyer, K.R., 1986. Coastal and Estuarine Sediment Dynamics. Wiley & Sons, Chichester. 342p.

Dyer, K.R., 1989. Sediment processes in estuaries: future research requirements. J. Geophys. Res. 94 (C10), 14327–14339.

Dyer, K.R., Cornelisse, J.M., Dearnaley, M., Jago, C., Kappenburg, J., McCave, I.N., Pejrup, M., Puls, W., van Leussen, W., Wolfstein, K., 1996. A comparison of in-situ techniques for estuarine floc settling velocity measurements. J. Sea Res. 36, 15–29.

Dyer, K.R., Christie, M.C., Feates, N., Fennessy, M.J., Pejrup, M., van Der Lee, W., 2000. An investigation into processes influencing the morphodynamics of an intertidal mudflat, the Dollard estuary, The Netherlands: I. Hydrodynamics and suspended sediment. Estuar. Coast. Shelf Sci. 50, 607–625.

Dyer, K.R., Bale, A.J., Christie, M.C., Feates, N., Jones, S., Manning, A.J., 2002a. The turbidity maximum in a mesotidal estuary, the Tamar estuary, UK. Part II: the floc properties. In: Winterwerp, J.C., Kranenburg, C. (Eds.), Fine Sediment Dynamics in the Marine Environment — Proc. in Mar. Sci, vol. 5. Elsevier, Amsterdam, pp. 219–232.

Dyer, K.R., Bale, A.J., Christie, M.C., Feates, N., Jones, S., Manning, A.J., 2002b. The turbidity maximum in a mesotidal estuary, the Tamar estuary, UK. Part I: dynamics of suspended sediment. In: Winterwerp, J.C., Kranenburg, C. (Eds.), Fine Sediment Dynamics in the Marine Environment — Proc. in Mar. Sci., vol. 5. Elsevier, Amsterdam, pp. 203–218.

Dyer, K.R., Christie, M.C., Manning, A.J., 2004. The effects of suspended sediment on turbulence within an estuarine turbidity maximum. Estuar.Coast. Shelf Sci. 59, 237–248.

EDF, 1998. TELEMAC-3D Version 2.2 — Manuel de Utilisateur, Report HE-42/97/048/B. Department Laboratoire National d'Hydraulique, EDF, France (in French).

Eisma, D., 1986. Flocculation and de-flocculation of suspended matter in estuaries. Neth. J. Sea Res. 20 (2/3), 183–199.

Fennessy, M.J., Dyer, K.R., Huntley, D.A., 1994a. INSSEV: an instrument to measure the size and settling velocity of flocs in-situ. Mar. Geol. 117, 107–117.

Fennessy, M.J., Dyer, K.R., Huntley, D.A., 1994b. Size and settling velocity distributions of flocs in the Tamar Estuary during a tidal cycle. Neth. J. Aquat. Ecol. 28, 275–282.

Fennessy, M.J., Dyer, K.R., Huntley, D.A., Bale, A.J., 1997. Estimation of settling flux spectra in estuaries using INSSEV. In: Burt, N., Parker, R., Watts, J. (Eds.), Proc. INTERCOH-1994: Cohesive Sediments. John Wiley & Son, Chichester, England, pp. 87–104.

Gibbs, R.J., Konwar, L.N., 1983. Sampling of mineral flocs using Niskin bottles. Environ. Sci. Technol. 17 (6), 374–375.

Gratiot, N., Manning, A.J., 2004. An experimental investigation of floc characteristics in a diffusive turbulent flow. In: Ciavola, P., Collins, M.B. (Eds.), Transport in European Estuaries. J. Coastal Res., vol. SI 41, pp. 105–113.

Hill, P.S., 1996. Sectional and discrete representations of floc breakage in agitated suspensions. Deep-Sea Res. 43, 679–702.

HR Wallingford, 2002. Estuary Process Research project (EstProc): Inception Report. Report prepared by the Estuary Process Consortium for the DEFRA and Environment Agency Joint Flood and Coastal Theme, Report No. FD1905/TR1. 53p.

Krone, R.B., 1963. A study of rheological properties of estuarial sediments. Report No. 63–68, Hyd. Eng. Lab. and Sanitary Eng. Lab. University of California, Berkeley.

Manning, A.J., 2001. A study of the effect of turbulence on the properties of flocculated mud. Ph.D. Thesis, Institute of Marine Studies, University of Plymouth, UK, 282p.

Manning, A.J., 2004a. The effects of turbulence on estuarine flocculation. In: Ciavola, P., Collins, M.B. (Eds.), Sediment Transport in European Estuaries. J. Coastal Res., vol. SI 41, pp. 70–81.

Manning, A.J., 2004b. Observations of the properties of flocculated cohesive sediment in three western European estuaries. In: Ciavola, P., Collins, M.B. (Eds.), Sediment Transport in European Estuaries. J. Coastal Res., vol. SI 41, pp. 90–104.

Manning, A.J., Dyer, K.R., 1999. A laboratory examination of floc characteristics with regard to turbulent shearing. Mar. Geol. 160, 147–170.

Manning, A.J., Dyer, K.R., 2002a. The use of optics for the in-situ determination of flocculated mud characteristics. J. Optics A, Pure App. Opt. 4, S71–S81 Institute of Physics Pub.

Manning, A.J., Dyer, K.R., 2002b. A comparison of floc properties observed during neap and spring tidal conditions. In: Winterwerp, J.C., Kranenburg, C. (Eds.), Fine Sediment Dynamics in the Marine Environment — Proc. in Mar. Sci., vol 5. Elsevier, Amsterdam, pp. 233–250.

Manning, A.J., Dyer, K.R., Christie, M.C., 2001. Properties of macroflocs in the lower reaches of the Gironde estuary. In: Elbee, J., Prouzet, P. (Eds.), Actes de VII$^{e}$ Colloque International de Oceanographie Du Golfe De Gascogne, Actes de Colloques No. 31. Ifremer, France, pp. 230–235.

Manning, A.J., Dyer, K.R., Lafite, R., Mikes, D., 2004. Flocculation measured by video based instruments in the Gironde estuary during the European Commission SWAMIEE Project. In: Ciavola, P., Collins, M.B. (Eds.), Sediment Transport in European Estuaries. J. Coastal Res, vol. SI 41, pp. 58–69.

Manning, A.J., Friend, P.L., Prowse, N., Amos, C.L., 2006. Preliminary findings from a study of Medway estuary (UK) natural mud floc properties using a laboratory mini-flume and the LabSFLOC system. Continental Shelf Research, BIOFLOW SI. doi:10.1016/j.csr.2006.04.011.

McCave, I.N., 1975. Vertical flux of particles in the ocean. Deep-Sea Res. 22, 491–502.

McCave, I.N., 1984. Erosion, transport and deposition of fine-grained marine sediments. In: Stow, D.A.V., Piper, D.J.W. (Eds.), Fine-Grained Sediments: Deep Water Processes and Facies, pp. 35–69.

Mehta, A.J., Partheniades, E., 1975. An investigation of the depositional properties of flocculated fine sediment. J. Hydrol. Res. 92 (C13), 361–381.

Nakagawa, H., Nezu, I., 1975. Turbulence in open channel flow over smooth and rough beds, Proc. Japan Soc. Civ. Eng. 241, 155–168.

Petersen, O., Vested, H.J., Manning, A.J., Christie, M.C., Dyer, K.R., 2002. Numerical modelling of mud transport processes in the Tamar Estuary. In: Winterwerp, J.C., Kranenburg, C. (Eds.), Fine Sediment Dynamics in the Marine Environment — Proc. in Mar. Sci., vol. 5. Elsevier, Amsterdam, pp. 643–654.

Prandle, D., Lane, A., Manning, A.J., 2005. Estuaries are not so unique. Geophys. Res. Lett. 32, L23614. doi:10.1029/2005GL024797.

Soulsby, R.L., 1983. The bottom boundary layer of shelf seas. In: Johns, B. (Ed.), Physical Oceanography of Coastal and Shelf Seas. Elsevier, New York, pp. 189–266.

Spearman, J., 2004. Note on the use of algorithms for modelling mud transport on tidal flats. HR Wallingford Ltd (UK) Tech. Report No. TR 144. 14p.

Stapleton, K.R., Huntley, D.A., 1995. Sea bed stress determinations using the inertial dissipation method and the turbulent kinetic energy method. Earth Surf. Processes. Landf. 20, 807–815.

Tolhurst, T.J., Gust, G., Paterson, D.M., 2002. The influence of an extracellular polymeric substance (EPS) on cohesive sediment stability. In: Winterwerp, J.C., Kranenburg, C. (Eds.), Fine Sediment Dynamics in the Marine Environment — Proc. in Mar. Sci., vol. 5. Elsevier, Amsterdam, pp. 409–425.

van Leussen, W., 1988. Aggregation of particles, settling velocity of mud flocs: a review. In: Dronkers, J., van Leussen, W. (Eds.), Physical Processes in Estuaries. Springer-Verlag, Berlin, pp. 347–403.

van Leussen, W., 1994. Estuarine macroflocs and their role in fine-grained sediment transport. Ph.D. Thesis, University of Utrecht, The Netherlands, 488p.

Winterwerp, J.C., 1999. On the dynamics of high-concentrated mud suspensions. Ph.D. Thesis, Delft University of Technology, Faculty of Civil Engineering and Geosciences, The Netherlands, 172p.

Winterwerp, J.C., 2006. On the sedimentation rate of cohesive sediment. In: Maa, J.P.-Y., Sanford, L.P., Schoellhamer, D.H. (Eds.), Coastal and Estuarine Fine Sediment Processes — Proc. in Marine Science, INTERCOH-2003. Elsevier, Amsterdam, pp. 203–220.

Winterwerp, J.C., Manning, A.J., Martens, C., de Mulder, T., Vanlede, J., 2006. A heuristic formula for turbulence-induced flocculation of cohesive sediment. Estuar., Coast. Shelf Sci. 68, 195–207.